Available online at www.sciencedirect.com
SCIENCE DIRECT
Journal of Power Sources 156 (2006) 424–433
JOURNAL OF POWER SOURCES
www.elsevier.com/locate/jpowsour

Main and interaction effects of PEM fuel cell design parameters

Galip H. Guvelioglu, Harvey G. Stenger *

Chemical Engineering Department, Lehigh University, Bethlehem, PA 18015, USA

Received 28 March 2005; received in revised form 3 June 2005; accepted 3 June 2005
Available online 28 July 2005

Abstract

In this work, a two-dimensional model is used to analyze the main and interaction effects of five design factors, at three levels in a polymer electrolyte membrane (PEM) fuel cell. The model used in this study is a detailed two-dimensional steady-state model, solved using a finite element partial differential equation solver. The factors considered are channel width, shoulder width, gas distribution electrode (GDE) thickness, GDE conductivity and GDE porosity. A full factorial design is used to minimize statistical errors and study interactions accurately. The model used is a two-dimensional, across-the-channel model. The model is run at both the inlet and exit concentrations for fuel and oxidant, allowing the study of interaction effects over a range of operating conditions. The analysis is conducted for operating potentials of 0.7 and 0.6 V and a range of current densities. The strongest interaction effects are found to exist between channel size and GDE conductivity, while the weakest interaction effects are between GDE thickness and GDE porosity.

Keywords: PEM fuel cell; Design of experiments; Factorial design; Interaction; Fuel cell design

1. Introduction

The interest in polymer electrolyte membrane (PEM) fuel cells for transportation, portable and stationary applications is growing as energy prices increase and concern for environmental impacts of internal combustion engines grows. Even though PEM fuel cells are conceptually simple electrochemical conversion devices, the underlying physics that describe their operation is complex. Since the early 1990's there have been a number of fundamental computational modeling studies directed towards understanding the complex physics of PEM fuel cell operation [1–4].

In recent years a general trend of using computational fluid dynamics (CFD) to model PEM fuel cells has evolved. Gurau et al. [5] developed the first realistic two-dimensional model of a fuel cell complete with flow channels and a fundamental representation of the membrane electrode assembly (MEA). Their along-the-channel model studied the effects of composition change of the reactants along the length of the channels. Um et al. [6] developed a two-dimensional transient, along-the-channel model and studied the change of current density with changing cell potential. Um and Wang [7] extended the work to the third geometric dimension and studied the effects of flow channel geometry and layout. A group at the Electrochemical Research Center of Pennsylvania State University developed a large-scale CFD model [8] and studied the two-phase transport issues in PEM fuel cells [9]. Berning et al. [10] developed a three-dimensional model, conducted parametric studies on operating pressure and temperature. They also studied geometrical variations and material properties [11], and developed a two-phase model [12].

Recently, Guvelioglu and Stenger developed a two-dimensional across-the-channel CFD PEM fuel cell model in which the effects of channel and bipolar plate shoulder dimensions as well as thickness and properties of fuel cell components were studied [13]. Even though the recent trend in PEM fuel cell modeling is 3D CFD models, the computational cost of accurate 3D modeling is large and not easily achievable. Typical anode and cathode catalyst layer thicknesses are on the order of 10–20 μm and the height and width of a single cell in a stack are 10–20 cm. These

* Corresponding author. Tel.: +1 610 758 4791; fax: +1 610 758 5057.
E-mail address: hgs0@lehigh.edu (H.G. Stenger).

0378-7753/$ – see front matter © 2005 Elsevier B.V. All rights reserved.
doi:10.1016/j.jpowsour.2005.06.009

Nomenclature

c_w	mass concentration of water in the membrane ($kg\,m^{-3}$)
p	pressure (Pa)
t	thickness (m)
x	mole fraction
V_{cell}	cell operating potential (V)
W	width (m)

Greek letters

σ	conductivity ($S\,m^{-1}$)
ε	porosity
ϕ	potential (V)

Subscripts

a	anode
c	cathode
ch	channel
GDE	gas distribution electrode
i	components, H_2 and H_2O for the anode and O_2, H_2O and N_2 for the cathode
l	liquid water
m	membrane
sh	shoulder
w	water in the membrane

Superscripts

0	boundary condition

dimension mismatches require more than a million elements to be used for even a small 7 cm × 1 cm section of a fuel cell, and take more than 1 h to solve with a 10–50 node parallel computer [8]. In this work, the two-dimensional across-the-channel domain enables the study of the design and operating conditions fast and efficiently, allowing the analysis of a wide range of design and operating parameters [13].

All of the CFD work of the previously cited authors was aimed towards increasing the understanding of fuel cell physics by simulating the performance of a given design. The work of Berning and Djilali [11] was a comprehensive study towards understanding the individual effects of various operating conditions, such as temperature, pressure and flow rates, together with design parameters like channel, shoulder lengths, gas distribution electrode porosity and thickness. Their work mostly focused on analyzing the effects of one variable at a time.

The major disadvantage of a one-factor strategy is that it fails to consider possible interactions between the factors studied. An interaction can be thought of as the failure of a factor to produce the same response at different levels of another factor. For example, in recent work [13], it was shown that the current density under the channel openings was lower than under the shoulders at moderate current densities when low conductivity electrode was used. However, with for higher electrode conductivity, the current density drop under the channels could be prevented. This behavior demonstrates an important interaction between channel size and conductivity of the electrode material on fuel cell performance. Another finding showed that high porosity electrodes improved performance for large channel and shoulder designs more than for smaller channel and shoulder designs. Thus, the effect of electrode porosity varies with design and illustrates interactions between porosity, channel size and shoulder size.

The design of PEM fuel cells is a complex problem. A PEM fuel cell consists of seven distinct regions:

- anode bipolar plate;
- anode gas distribution electrode layer;
- anode catalyst layer;
- membrane;
- cathode catalyst layer;
- cathode gas distribution electrode layer;
- cathode bipolar plate.

The design must have the right components for each region to meet the application requirements. The review of PEM fuel cell design and manufacturing by Mehta and Cooper [14] recommended 16 different polymer electrolyte membranes, 2 types of gas diffusion electrodes, 8 types of anode catalysts, 4 types of cathode catalysts and over 100 bipolar plate designs for further study.

Studying experimentally all possible combinations at all possible operating conditions is unrealistic, however, it is realistic to conduct a well designed factorial set of experiments. In this work, the following five different PEM fuel cell design parameters are studied:

- bipolar plate channel size;
- bipolar plate shoulder size;
- gas distribution electrode thickness;
- porosity of the gas distribution electrode;
- conductivity of the gas distribution electrode.

The model can vary these design parameters for both anode and cathode, however, to simplify the analysis, this work will use the identical parameters for both the anode and cathode.

2. Model description

The model used in this design of experiments analysis was published earlier [13]. It assumes:

- steady-state operation;
- isothermal operation;
- ideal gas mixtures;
- single phase mode;
- isotropic and homogeneous electrodes and membrane;

- the membrane is considered impermeable for the gas phase;
- negligible contact resistance;
- minimal membrane swelling.

The anode and cathode catalyst layers are modeled as reactive boundaries because their thickness of 10–25 μm is significantly smaller than all other component thicknesses. The PEM fuel cell model is a comprehensive two-dimensional, isothermal, steady-state model providing a detailed description of the following transport phenomena:

- multi-component flow;
- diffusion of reactants through the porous electrodes;
- electrochemical reactions;
- transport of electrons through the electrodes;
- water balance in the membrane.

The equations governing these processes include:

- ionic balance in electrodes and membrane;
- the Maxwell–Stefan equations for multi-component diffusion and convection in gas distribution channels and gas distribution layers;
- Darcy's law for the flow of species in porous electrodes;
- water balance and water flux in the membrane governed by diffusion, convection and electro-osmotic drag.

FEMLAB®, a finite element computational fluid dynamics package, was used to solve the non-linear system of equations. The model was first created and tested in FEMLAB's® graphical user interface and then saved as a MATLAB® m-file [15]. Details of the model, geometry meshing and solver settings were presented in Guvelioglu and Stenger [13]. The typical run times for the 2D simulation was 30–300 s per design. The longer times being for high current density operations. The majority of the runs were completed under 150 s on an Intel Pentium® 4, 3.2 GHz CPU with 1 GB of DDRam.

3. Design and analysis of experiments

The first step in this analysis is to identify the factors and their range of variation, which requires a fundamental understanding of the physics of the process. After the factors and the levels are identified, the method of design is selected depending on the resources available to conduct the experiments. There are several experimental designs that can be selected: full factorial, fractional factorial and Taguchi designs [16].

In a full factorial experiment, responses are measured at all combinations of the factor levels, which may result in a prohibitive number of runs. For example, a two-level full factorial design with 6 factors requires 64 runs (2^6) and a two level design with 9 factors requires 512 runs (2^9). To minimize time and computational cost, factorial designs that exclude some of the factor level combinations can be used. However, choosing the best fraction often requires specialized knowledge of the process under investigation.

Table 1
Design factors studied and their values

Parameter	Low	Middle	High
W_{ch}, the gas channel width (m)	0.5×10^{-4}	1.0×10^{-3}	2.0×10^{-3}
W_{sh}, the bipolar shoulder width (m)	0.5×10^{-4}	1.0×10^{-3}	2.0×10^{-3}
t_{GDE}, Anode and cathode GDE thickness (m)	1.5×10^{-4}	3×10^{-4}	4.5×10^{-4}
ε_{GDE}, GDE porosity of the anode and cathode	0.4	0.5	0.6
σ_{GDE}, GDE conductivity ($S\,m^{-1}$)	200	570	1000

A full factorial design has the advantage that even though the number of runs is greater, it will find interactions which can avoid misleading conclusions and the interactions are valid over the range of experimental conditions. In this work, to minimize statistical errors and to study interactions fully, a factorial design is selected with five design factors at three levels (see Table 1). The three levels are selected such that "current technology" is bounded by a lower and higher value.

Fig. 1 shows the design factors studied, their physical meanings, and the domains where they are active. The factors and the levels, shown in Table 1, yield 243 runs (3^5), for each of the four operating conditions (0.6 and 0.7 V at the entrance and exit conditions). These 243 experiments were run and the results were analyzed with the commercial statistical package MINITAB® [17].

4. Results and discussion

4.1. Model validation

The fuel cell design parameters used to validate the model are shown in Table 2. They are based on the work of Um and Wang [7]. The 2D computational domain used allows the channel and shoulder width effects to be studied in detail; however, because it is not a 3D model it cannot study the concentration changes along-the-channel. Fuel cells are typically operated with some excess hydrogen and oxygen [7], which means the concentration of reactants will not be zero at the exit. However, the concentration changes are large enough to lower the average current density of the fuel cell. To assess concentration change effects, two different fuel and oxidant conditions are considered; one at the entrance and the other at exit of the fuel cell. Fully humidified hydrogen and air

Table 2
Base case geometric parameters

Parameter	Value
W_{ch}, the gas channel width (m)	7.62×10^{-4}
W_{sh}, the bipolar shoulder width (m)	7.62×10^{-4}
t_{GDE}, Anode and cathode GDE thickness (m)	3×10^{-4}
t_m, Membrane thickness (m)	1.78×10^{-4}
ε_{GDE}, GDE porosity of the anode and cathode	0.6

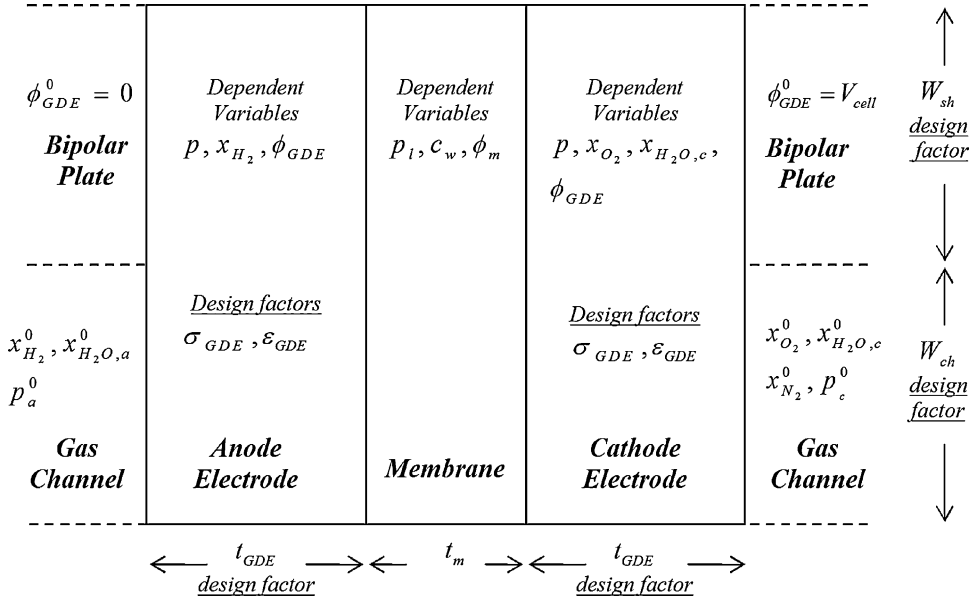

Fig. 1. The computational domain, dependent variables and design factors.

are used at the entrance conditions while the exit conditions are calculated by assuming 50% excess hydrogen and oxygen and based on a 1 A cm^{-2} current density. The water flux between the anode and cathode sides was neglected when calculating the exit water compositions.

The compositions and conditions used in validating the model are shown in Table 3, and Fig. 2 shows the fuel cell performance curve at the entrance and exit of the fuel cell. The performance curve for the entrance conditions (Fig. 2) shows a good agreement with experimental results reported by Um and Wang [7] at current densities below 0.3 A cm^{-2}, for higher current densities the model over-predicts the performance. This is expected since the concentrations are not at the entrance values for the entire fuel cell. The model at the exit conditions under-predicts the experimental results at low current densities but shows good agreement at high current densities. The overall average fuel cell performance is expected to fall between the entrance and exit performance curves of Fig. 2, which shows that the model does predict the fuel cell performance accurately. The kinetic parameters used in this model were not adjusted to fit this performance curve but are the same parameters used previously in an earlier study [13], which was at pressures of 3 atm at the anode and 5 atm at the cathode.

Table 3
Operating condition parameters

Symbol	Value
T, temperature (K)	343.15
p^0_a, Anode side pressure (Pa)	202650
p^0_c, Cathode side pressure (Pa)	202650

	Entrance conditions	Exit conditions
$x^0_{O_2}$, Cathode feed oxygen mole fraction	0.178	0.053
$x^0_{H_2O,c}$, Cathode feed water mole fraction	0.154	0.349
$x^0_{N_2}$, Cathode feed nitrogen mole fraction	$1 - x^0_{O_2} - x^0_{H_2O,c}$	$1 - x^0_{O_2} - x^0_{H_2O,c}$
$x^0_{H_2}$, Anode feed hydrogen mole fraction	0.846	0.647
$x^0_{H_2O,a}$, Anode feed water mole fraction	$1 - x^0_{H_2}$	$1 - x^0_{H_2}$

4.2. Main effects of design factors

Figs. 3–6 show the main effects of the design factors on the mean current density for operating potentials of 0.7 and

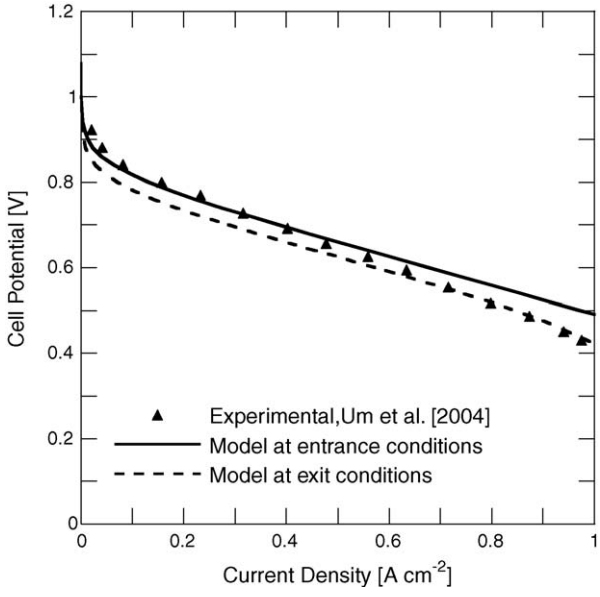

Fig. 2. Comparison of the model at the entrance and exit conditions with an experimental polarization curve.

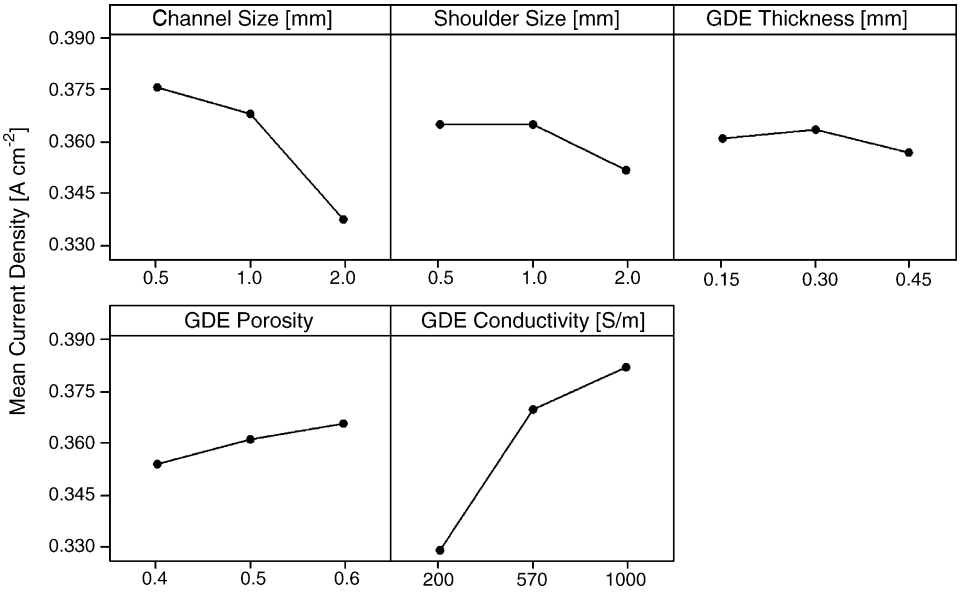

Fig. 3. Main effect plots for cell operating at 0.7 V, at the entrance conditions.

0.6 V at the entrance and exit conditions. Fig. 3 is for the case of 0.7 V at the entrance conditions, Fig. 4 is at 0.7 V and exit conditions and Figs. 5 and 6 are for 0.6 V at the entrance and exit conditions, respectively.

Operating at 0.7 V at the entrance conditions, the fuel cell mean current density increases as the channel size decreases as shown in Fig. 3. Reducing the channel size from 2 to 1 mm increases the current density by 9%. Further reducing it to 0.5 mm increases the current density by only 2%. Thus, the gain in current density might not be worth the increase in compressor duties needed for pressure drop in the smaller channels. For the cell operating at 0.7 V and the exit conditions (Fig. 4), the reduction of channel size from 2 to 1 mm and from 1 to 0.5 mm results in 7.5 and 0.5% increase in current densities.

At 0.7 V at the entrance conditions (Fig. 3), reducing the shoulder size from 2 to 1 mm improves the cell performance by 3.8%, while further reducing it to 0.5 mm does not improve the performance. Thus, below 1 mm the transport of reactants under the bipolar plate shoulders does not appear to be rate limiting. However, at the exit of the cell where the reactant concentrations are lower, decreasing the shoulder size overcomes the mass transport limitations of reactants under the shoulders, which causes a current density increase. When the cell is operated at 0.6 V, and a higher mean current density, more reactants need to be transported to the catalyst. Benefits

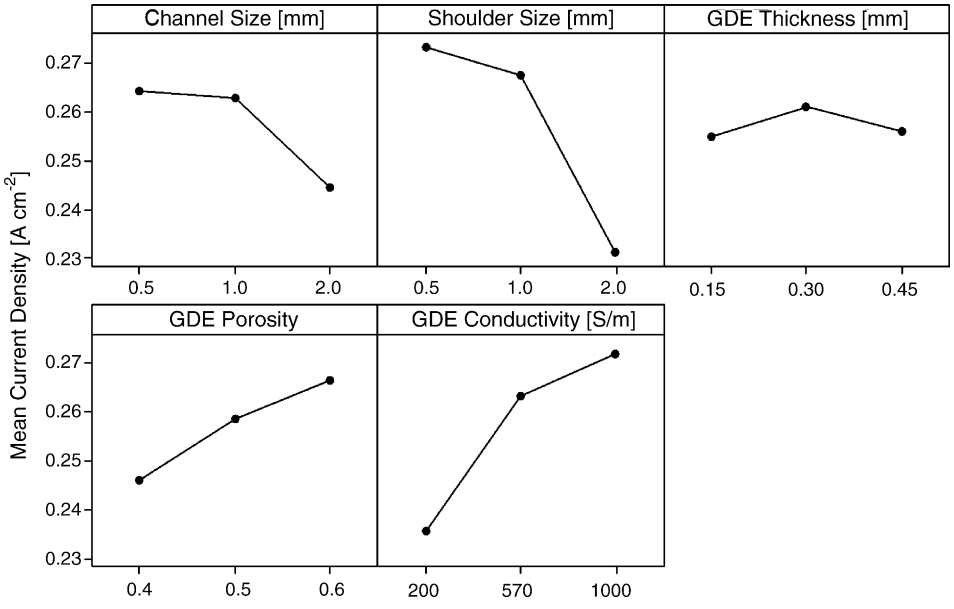

Fig. 4. Main effects for cell operating at 0.7 V, at the exit conditions.

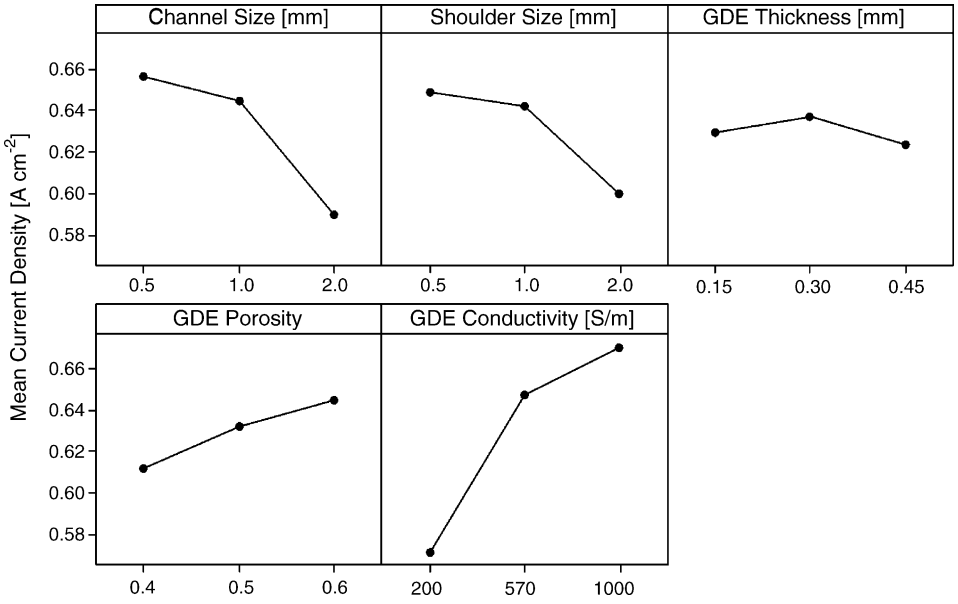

Fig. 5. Main effects for cell operating at 0.6 V, at the entrance conditions.

from reducing the shoulder size, is seen even at the entrance condition (Fig. 5).

The main effects of the gas distribution electrode (GDE) thickness, shows that a maximum current density is reached at a thickness of 0.3 mm, for all operating cases. Electrodes that are too thin or too thick lower the mean current density. The magnitude of the GDE thickness, main effect, is about ±2%, significantly less than other main factors. However, analyzing just the main effect of the GDE thickness might lead to incorrect conclusions if other interactions are neglected.

For both 0.7 and 0.6 V cell potentials and for both entrance and exit conditions, increasing the porosity of the electrode increases the mean current density. The effect of increasing GDE porosity from 0.4 to 0.6 increases the mean current density by 3.3 and 8.5% for 0.7 V cell potential at the entrance and exit conditions, respectively. For high current density operation (0.6 V) the porosity effect is more significant and results in 5.5 and 16% increases for entrance and exit conditions, respectively. Clearly, the GDE porosity is a key design parameter. As the reactants are consumed and their concentrations decrease, the porosities of the GDE's become more important.

The base case electrode conductivity of 570 S m^{-1} was estimated from commercial electrode properties and is similar to the estimate of Nguyen et al. [18]. Nearly, doubling the

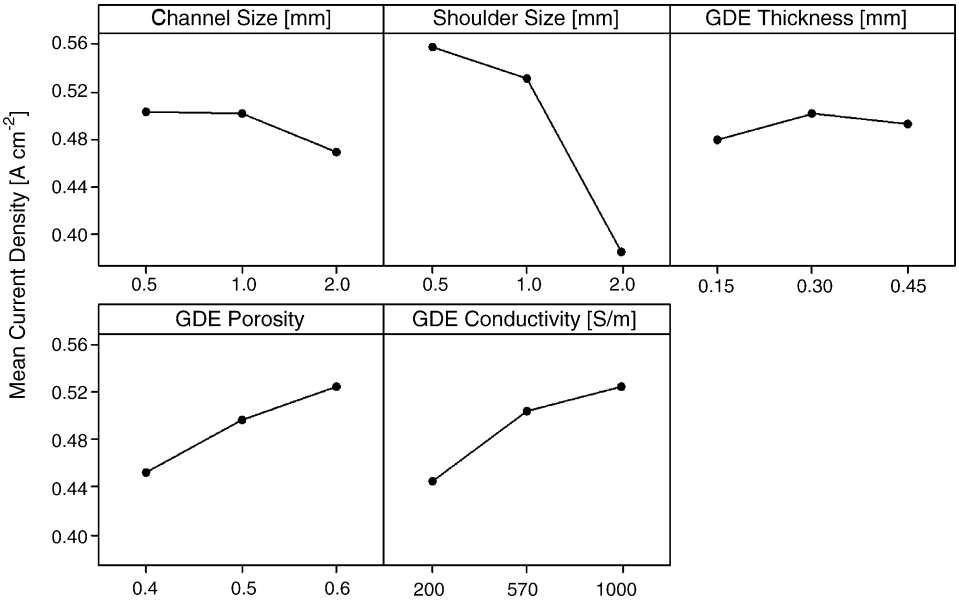

Fig. 6. Main effects for cell operating at 0.6 V, at the exit conditions.

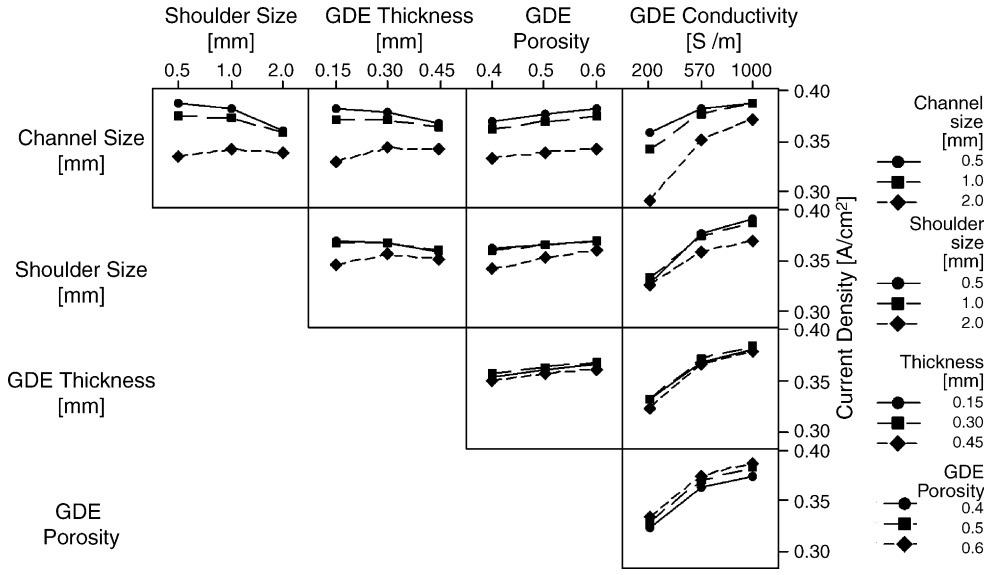

Fig. 7. Interaction plots for cell operating at 0.7 V, at the entrance conditions.

conductivity (570–1000 S m^{-1}) yields an increase in current density of 3.2–4.1% for all four operating cases. When the conductivity of the GDE is reduced to 200 S m^{-1}, the mean current densities decrease by 10.5–11.7%.

Four of the five design factors significantly changed the performance of the fuel cell. The fifth factor, GDE thickness, was found to have a minimal impact. However, ruling out GDE thickness as a critical design factor may be incorrect when considering its interaction with other factors.

4.3. Interactions between design factors

The major disadvantage of the one factor strategy is that it fails to consider possible interactions between the factors. Figs. 7–10 show the interaction plots for the five design parameters. Significant interaction is indicated by non-parallel lines in each plot. For example the first row, first column plot in Fig. 7 identifies strong interactions between channel and shoulder dimensions through the lack of parallelism of the lines. For a 1 mm channel size an increase in mean current densities is observed when the shoulder is reduced from 2 to 1 mm. However, the rate of increase in current density is not as large as the 0.5 mm channel case. When the shoulder size is reduced from 1 to 0.5 mm, no change in mean current density can be observed for the 2 mm channel contrary to 0.5 mm channel case. This lack of parallelism between the lines shows that there is interaction between channel and shoulder size effects. The interactions between

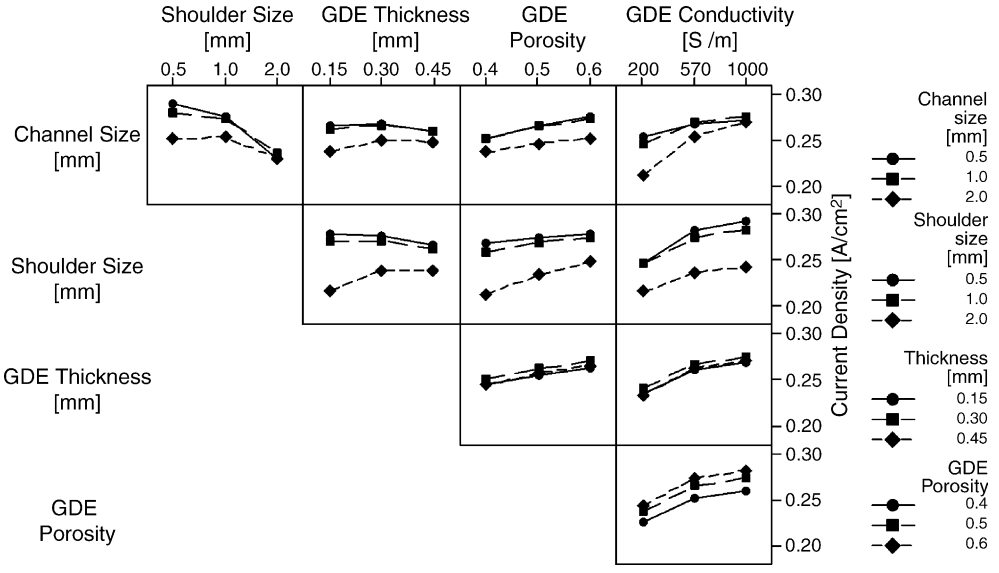

Fig. 8. Interaction plot for cell operating at 0.7 V, at the exit conditions.

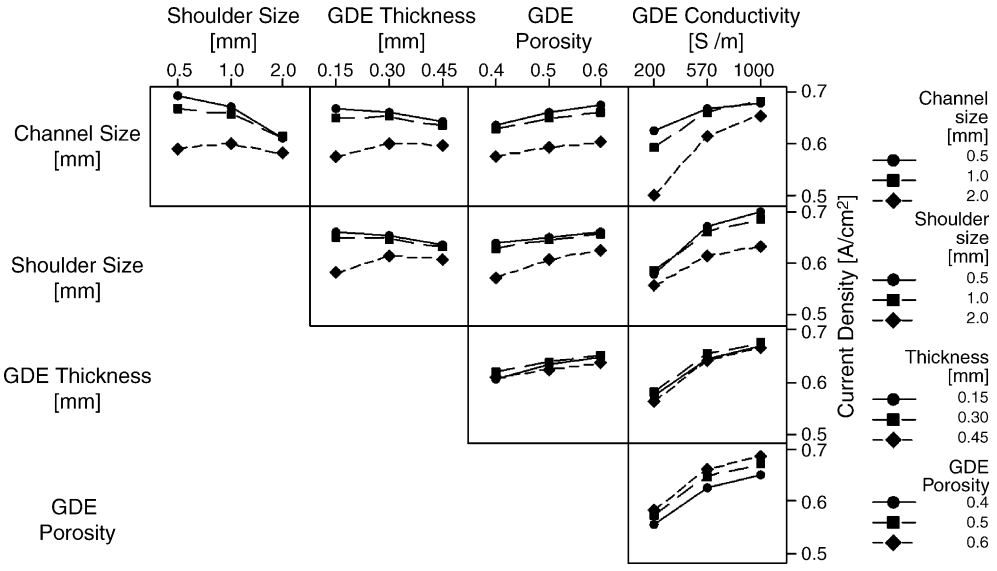

Fig. 9. Interaction plot for cell operating at 0.6 V, at the entrance conditions.

channel and shoulder effects are even more visible for 2 mm channel size; where reducing the shoulder size from 2 to 1 mm increases the mean current density slightly while further reducing the shoulder size actually results in a slight decrease in mean current density.

When Figs. 7–10 are analyzed, it is clear that the strong interactions between the design factors that are present for 0.7 V at entrance conditions (Fig. 7) are also visible for the other three operating conditions. The observed interactions and their qualitative magnitudes for all four operating conditions studied are summarized in Table 4. The interactions observed for the entrance conditions are also visible for the exit conditions. Also the interactions seen for 0.7 V operation are valid for the 0.6 V operation but with increased magnitudes.

The interactions between GDE thickness and channel are strong and are observed for all channel sizes. However, for GDE thickness and shoulder size, minimal interaction is observed for both 0.5 and 1 mm shoulders. The interaction between shoulder and GDE thickness become more visible for 2 mm shoulder size.

Strong interactions between GDE conductivity and channel sizes can be observed for all four operating conditions. When larger channels are used, performance increase is obtained using GDE's with higher conductivity. The GDE conductivity interactions with the shoulder sizes are mild and are only observed for 2 mm shoulders.

Strong interaction between GDE porosity and shoulder size effects are observed for 2 mm channels but no interaction for smaller shoulders is identified. For the operation of PEM

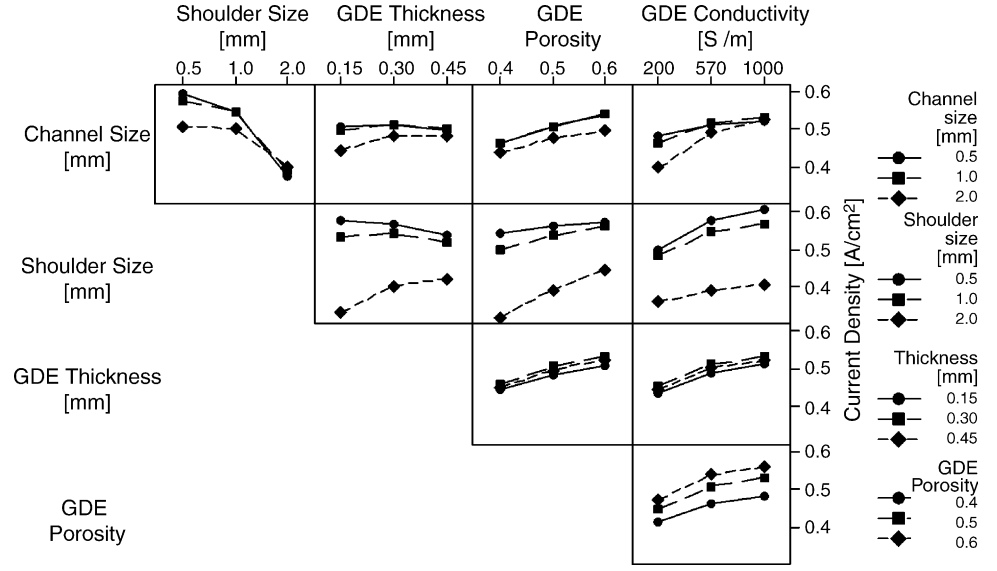

Fig. 10. Interaction plot for cell operating at 0.6 V, at the exit conditions.

Table 4
Summary of interactions between factors

	Shoulder	GDE thickness	GDE porosity	GDE conductivity
Channel	Strong	Strong	Mild	Strong
Shoulder	–	Strong	Strong	Mild
GDE thickness	–	–	Negligible	Negligible
GDE porosity	–	–	–	Negligible

fuel cells, the GDE porosity is an important factor as shown in earlier sections when main effects were discussed. The porous electrodes must allow transport of the reactants to the catalyst sites, thus increasing GDE porosity improves the performance of the PEM fuel cells more for larger shoulder designs, as the transport of the reactants to the catalyst sites under the shoulders becomes more difficult.

The interaction of GDE porosity with channel size is small at low current density (higher voltages) and at the entrance conditions where the mass transport is not rate limiting; however, as the current density increases (voltage decreases) or as the concentrations decrease, the interactions are slightly more visible. The GDE porosity and GDE thickness interaction is very small compared to the interactions discussed previously and can be neglected. Also at the operating conditions studied there is no evidence of interaction between GDE porosity and GDE conductivity or between GDE thickness and GDE conductivity.

5. Conclusions

Design of PEM fuel cells is a complex problem with a wide range of choices for fuel cell components [14]. Although running experiments testing all combinations of these components would be prohibitively costly, recent developments in mathematical modeling make it possible to rapidly evaluate PEM fuel cell designs at various operating conditions. In this study, a two-dimensional CFD based mathematical model is used to evaluate different design factor effects on the performance of a PEM fuel cell.

Design of experiments analysis is a useful and efficient approach to identify the interactions between design factors. This is the first study to use design of experiments analysis with a PEM fuel cell model to study the interaction effects between design factors. When a one factor at a time approach is used, the interactions between design factors cannot be identified and wrong conclusions can be drawn about the effects of factors. For example, the main effects of the GDE thickness showed that changing the thickness alone does not improve the performance significantly. Thus, if the GDE thickness is studied in a one factor at a time study, the researcher could have concluded that the GDE thickness is not a critical factor in PEM fuel cell design. However, the interaction between GDE thickness, shoulder size and channel sizes are clear and important. Also the interactions between design factors change with cell potential and concentrations of the reactants. Some interactions appear only for certain values of design factors, thus increasing the complexity of PEM fuel cell design and operation. When the entrance and exit conditions are compared, it is found that the interactions between design factors effecting mass transport become more visible. These interactions are greater for a cell operating at 0.6 V, since the rate of reaction is faster and more reactants need to be transported to the catalyst sites.

A full factorial design of experiments was successfully used in this study due to the relatively small size of the problem, 243 runs for each operating condition. The applicability of a full factorial design was made possible by the speed and robustness of the model used in the calculations. Each run took about 2–3 min, thus the 243 runs were completed in less than 12 h using a desktop PC. If a three-dimensional CFD model were used, the full factorial design would be computationally demanding as the typical run times are on the order of hours. By repeating the interaction analysis at the exit concentrations it is shown that interactions between design factors do not change dramatically, except for slight increases in existing interactions effecting mass transport. Therefore, a two-dimensional model can capture the significant interactions between design parameters.

Acknowledgements

We would like to thank Pinar Keles from Lehigh University and Dr. Sanjay Mehta from Air Products and Chemicals Inc., for their contributions on the analysis of the results.

References

[1] D.M. Bernardi, M.W. Vebrunge, A mathematical model of the solid-polymer-electolyte fuel cell, J. Electrochem. Soc. 139 (9) (1992) 2477–2491.
[2] T.E. Springer, T.A. Zawodzinski, S. Gottesfeld, Polymer electrolyte fuel cell model, J. Electrochem. Soc. 138 (8) (1991) 2334–2342.
[3] T.F. Fuller, J. Newman, Water and Thermal management in solid polymer electrolyte fuel cell, J. Electrochem. Soc. 140 (5) (1993) 1218–1225.
[4] J.J. Baschuk, X. Li, Modeling of polymer electrolyte membrane fuel cells with variable degrees of water flooding, J. Power Sources 86 (2000) 181–196.
[5] V. Gurau, H. Liu, S. Kakac, Two-dimenisonal model for proton exchange membrane fuel cells, AIChE J. 44 (11) (1998) 2410–2422.
[6] S. Um, C.-Y. Wang, K.S. Chen, Computational fluid dynamics modeling of proton exchange membrane fuel cells, J. Electrochem. Soc. 147 (12) (2000) 4485–4493.

[7] S. Um, C.Y. Wang, Three-dimensional analysis of transport and electrochemical reactions in polymer electrolyte fuel cells, J. Power Sources 125 (2004) 40–51.
[8] H. Meng, C.Y. Wang, Large-scale simulation of polymer electrolyte fuel cells by parallel computing, Chem. Eng. Sci. 59 (2004) 3331–3343.
[9] U. Pasaogullari, C.Y. Wang, Two-phase transport and the role of micro-porous layer in polymer electrolyte fuel cells, Electrochem. Acta 49 (2004) 4359–4369.
[10] T. Berning, D.M. Lu, N. Djilali, Three-dimensional computational analysis of transport phenomena in a PEM fuel cell, J. Power Sources 106 (2002) 284–294.
[11] T. Berning, N. Djilali, Three-dimensional computational analysis of transport phenomena in a PEM Fuel Cell—a parametric study, J. Power Sources 124 (2003) 440–452.
[12] T. Berning, N. Djilali, A 3D, multiphase, multicomponent model of the cathode and anode of a PEM fuel cell, J. Electochem. Soc. 150 (12) (2003) A1598–A1607.
[13] G.H. Guvelioglu, H.G. Stenger, Computational fluid dynamics modeling of polymer electrolyte membrane fuel cells, J. Power Sources 147 (2005) 95–106.
[14] V. Mehta, J.S. Cooper, Review and analysis of PEM fuel cell design and manufacturing, J. Power Sources 114 (2003) 32–53.
[15] MATLAB 7.0, The MathWorks Inc., Natick, MA, 2004.
[16] D.C. Montgomery, Design and Analysis of Experiments, fifth ed., Wiley, New York, 2001.
[17] Minitab Inc., MINITAB User's Guide, Release 14, 2004.
[18] P.T. Nguyen, T. Berning, N. Djilali, Computational model of a PEM fuel cell with serpentine gas flow channels, J. Power Sources 130 (2004) 14–157.